metals

MDPI

Article

Study of the Microstructure, Tensile Properties and Hardness of AZ61 Magnesium Alloy Subjected to Severe Plastic Deformation

Ondřej Hilšer [1,*], Stanislav Rusz [1], Pavel Szkandera [1], Lubomír Čížek [2], Martin Kraus [2], Jan Džugan [3] and Wojciech Maziarz [4]

1 Department of Mechanical Technology, Faculty of Mechanical Engineering, VSB-Technical University of Ostrava, 17. listopadu 15/2172, 708 33 Ostrava-Poruba, Czech Republic; stanislav.rusz@vsb.cz (S.R.); pavel.szkandera.st@vsb.cz (P.S.)

2 Department of Materials Engineering, Faculty of Metallurgy and Materials Engineering, VSB-Technical University of Ostrava, 17. listopadu 15/2172, 708 33 Ostrava-Poruba, Czech Republic; lubomir.cizek@vsb.cz (L.Č.); martin.kraus@vsb.cz (M.K.)

3 COMTES FHT Inc., Průmyslová 995, 334 41 Dobřany, Czech Republic; jan.dzugan@comtesfht.cz

4 Institute of Metallurgy and Materials Science, Polish Academy of Sciences, Reymonta Street 25, 30-059 Kraków, Poland; w.maziarz@imim.pl

* Correspondence: ondrej.hilser@vsb.cz; Tel.: +420-597329412

Received: 22 August 2018; Accepted: 26 September 2018; Published: 28 September 2018

Abstract: Hot extruded (EX) AZ61 magnesium alloy was processed by the twist channel angular pressing (TCAP) method, which combines equal channel angular pressing (ECAP) and twist extrusion (TE) processes and significantly improves the efficiency of the grain refinement process. Both the initial hot extruded AZ61 alloy and the alloy after completion of TCAP processing were examined by using optical microscopy (OM), scanning electron microscopy (SEM), transmission electron microscopy (TEM) and electron backscatter diffraction (EBSD) and their corresponding micro-tensile testing (M-TT) and hardness testing at room temperature. The results showed that the microstructure of hot extruded alloy was refined well by TCAP due to dynamic recrystallization (DRX) caused by TCAP. The tensile properties, investigated by micro-tensile testing (M-TT), of the AZ61 alloy were significantly improved due to refined microstructure. The highest tensile properties including YS of 240.8 MPa, UTS of 343.6 MPa and elongation of 21.4% of the fine-grained alloy with average grain size below 1.5 μm was obtained after the third TCAP pass at 200 °C using the processing route B_c.

Keywords: severe plastic deformation; ECAP; twist extrusion; hot extruded AZ61; structure; tensile properties; hardness

1. Introduction

The low mass of magnesium alloys causes that they are more readily used, where mass reduction of various types of components while maintaining mechanical and functional parameters is important, desirable, and cost-effective. The development of new design trends relies on optimizing work conditions, reduction of energy consumption, and recycling opportunities; it allows an assessment that the world usage of magnesium alloys will increase steadily over the next few years, which means that a greater amount of products and components will be made from this material. According to statistics [1], the production of magnesium alloy castings increased between 1993 and 2003 in parabolic to nearly 180,000 tons and Europe had a significant share of this increase approx. 80,000 tons). Data published by the US Geological Survey indicate that China's primary magnesium production in 2011 amounted to 670,000 tons as early as 2002, the amount of magnesium produced in China

accounted for half of the worlds magnesium production; by 2013, it increased to 75% of the world market. The share in the United States was approx. 63,000 tons; in other countries, it was approx. 110,000 tons [2].

A combination of good specific strength with relatively low density (1.74 g/cm^3) has largely contributed to the use of magnesium alloys for fast moving parts, where violent speed variations occur and where the weight reduction of the final products is required. The largest need for magnesium alloys has been shown and is still in the automotive industry (approx. 70%). The pursuit of modern designers for the construction of light-weight vehicles and consequently of low fuel consumption, has contributed to the use of magnesium alloys as a construction material for automotive wheels, engine pistons, gearboxes and clutch housings, roof window frames, door constructions, pedals, suction channels, manifolds, drive shafts, differential mechanisms, brackets, radiators, and more. The growing tendencies for an ever-increasing use of magnesium alloys motivate research and academic sphere to work intensively in order to find out new solutions for this group of materials in areas not only of the automotive or sports industries, but also, and perhaps more, in more advanced areas, in biomedical engineering, which enables the production of new generation materials capable of meeting the increased demands placed by manufacturers and ultimately also consumers [2].

Due to the high industrial requirements coming mainly from the low density of Mg alloys and the high availability of Mg of approx. 2% of the earth's crust [3], and the fact that magnesium alloys are characterized by good vibration damping ability, the greatest among all currently known construction materials and high dimensional stability, the research issues focused on these alloys are interesting both at the research and application level [4].

Great properties of this group of materials also make it possible to optimize the design process of the constructed elements, due to their reliability and functional properties of the final product [4,5]. Modern casting technologies and plastic deformation methods provide good external surface quality of magnesium alloys, durability, and reliability in service conditions, as well as high dimensional stability, which makes Mg alloys increasingly popular and their use justified not only from the technological point but also from economic of view.

Among the currently developed technologies of plastic deformation of metallic materials, severe plastic deformation (SPD) methods are worth to mention. This plastic deformation technologies consists of transforming the micrometric structure of coarse-grained materials into ultra-fine (UFG with grain size 100–1000 nm) and/or nanometric materials (grain size < 100 nm) by re-organizing the dislocation structure created during plastic deformation [5,6]. Standard examples of methods of severe plastic deformation are ECAP [7–9], High-Pressure Torsion (HPT) [10], Accumulative Roll Bonding (ARB) [11], Cyclic Extrusion Compression (CEC) [12], or Hydrostatic Extrusion (HE) [13]. Severe plastic deformation methods in contrast to conventional technologies of plastic deformation are not used to shape the initial material, but primarily to transform the coarse-grained microstructure into ultra-fine or nanometric microstructure [14]. The obtained grain size and nature of the produced nanostructures depend mainly on: SPD process conditions, phase composition, and initial grain size of the starting material. Compared to the conventional (coarse-grained) materials that were subjected to SPD processing they are characterized by greater mechanical and physical properties [14,15].

2. The Effect of TCAP Processing

The manuscript presents the influence of severe plastic deformation by using the TCAP (twist channel angular pressing) as a method for increasing the efficiency of SPD. The horizontal part of the TCAP channel is manufactured into a helix shape with an angle of lead $\gamma = 30^\circ$, the TCAP die geometry thus combines the conventional ECAP method and the TE [16] method. The influence of the TCAP channel design was presented by Rusz or Greger in the papers [17,18]. The effect of TCAP geometry on the grain refinement of Al-Mg-based alloys was verified by Snopiński et al. [19]. Figure 1 shows an illustration of ECAP and TCAP die design.

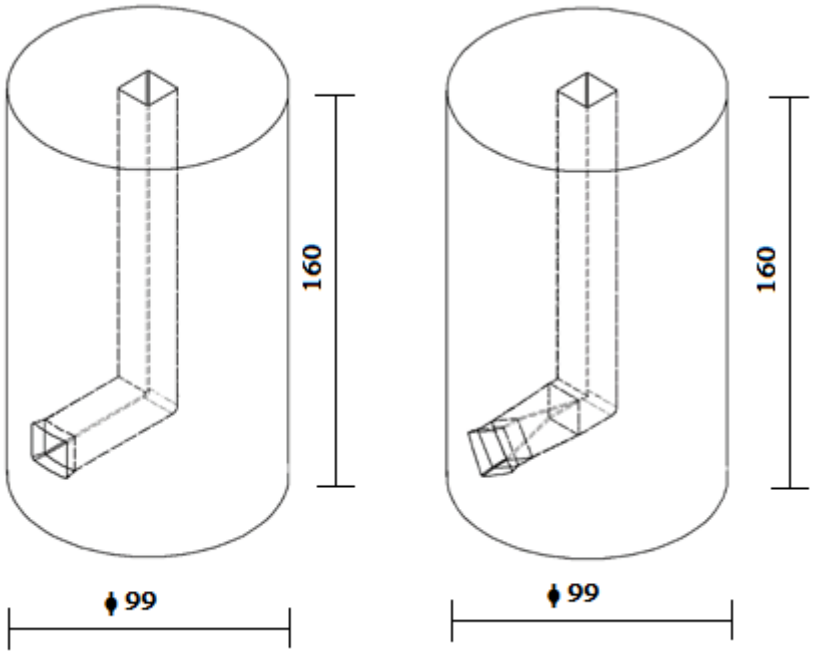

Figure 1. Schematic illustration of the equal channel angular pressing (ECAP) die channel: conventional ECAP geometry (**a**); ECAP geometry with the helical horizontal channel, i.e., twist channel angular pressing (TCAP) (**b**).

During extrusion of an experimental sample with the use of a tool with modified geometry, the refining starts with shearing strain originated during the passes through the deformation zone, which is at the place of transition from the vertical position to the horizontal position of the TCAP extrusion channel. This part of the process is identical with the conventional ECAP process. After the sample passes through the deformation zone, the sample is then extruded into the helix. The effect of the helix in the horizontal part of the channel lies in the fact that the sample in the first stage is decelerated, which means it encounters a back pressure (BP). For continuation of the forming process, it is necessary to increase the extrusion force, and this leads to an increase of strain intensity. By using this geometry of extrusion channel, it is possible to obtain a value of strain intensity of ~1.35 (Figure 2a). In the case of a conventional geometry of the channel, the value of plastic strain intensity is ~1.05 (Figure 2b).

The positive effect of twist channel angular pressing (TCAP) allows us the following:

- the increase of the value of the introduced strain and thus the possibility of reducing the necessary number of passes necessary for achieving the UFG structure,
- the resulting back pressure allows extrusion of materials crystallising in hcp lattice, which are typically characterised by low plasticity and during extrusion by the ECAP method a cracking of the sample would most likely occur due to a limited number of slip systems,
- homogeneous distribution of effective plastic strain (refined grains), in comparison with conventional geometry, see Figure 2,
- elimination of occurrence of the so-called "Dead zone".

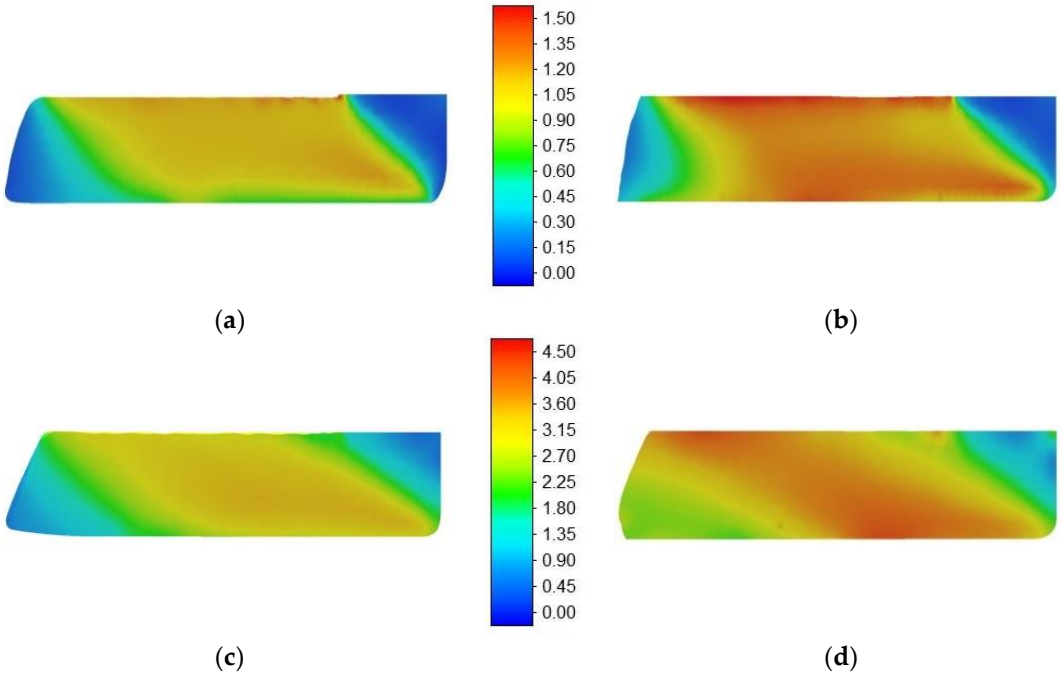

Figure 2. The effective plastic strain distribution after ECAP and TCAP processing in longitudinal direction: (**a**) after the first ECAP pass; (**b**) after the first TCAP pass; (**c**) after the third ECAP pass; and (**d**) after the third TCAP pass.

3. Experimental Material and Procedure

The experiments were concentrated on the influence of severe plastic deformation method TCAP on the grain refinement and tensile properties of hot extruded (at 430 °C) magnesium alloy AZ61. The investigated material was supplied by the Institute of Non-ferrous Metals in Gliwice, Department of Light Metals (OML Skawina), Poland. The chemical composition of the experimental alloy is presented in Table 1.

Table 1. The chemical composition of the AZ61 magnesium alloy (in wt.%).

Material	Fe	Si	Mn	Ni	Cu	Zn	Al	Mg
AZ61	0.003	0.030	0.230	0.001	0.003	1.092	6.430	rest

An advantage of using the samples in the extruded initial state is the refinement of the cast grain having an average size of ~100 μm to a size of ~24 μm. We can assume that by using the initially extruded state of the samples, the number of TCAP passes necessary for the achievement of the desired refinement and homogeneity of the structure, can be reduced.

Due to the limited formability of investigated alloy at low temperature (below 200 °C), the extruded alloy AZ61 was deformed by the TCAP method at a temperature of 200 °C (the temperature is the same for the sample and the channel) with the constant deformation rate of 40 mm/min. Samples were rotated by 90° around the longitudinal axis (Bc processing route). In view of our already published results that were focused on the use of the TCAP channel, an experimental realization of TCAP process was proposed that involved the execution of a maximum of three passes by the TCAP method. During the extrusion of the individual samples of the investigated alloy AZ61, it is possible to measure the dependence of the flow stress of the extruded sample on the path by means of a strain gauge sensor mounted on a cylinder of a hydraulic press DP 2000. The resulting curve serves as the primary indicator of the effect of TCAP on changes of structure in the sample subjected to a TCAP process.

Microstructural analysis of investigated magnesium alloy was realized on the NEOPHOT 2, optical microscope (VŠB-Technical university of Ostrava, Ostrava, Czech Republic). Detailed study

of the severely plastic deformed structure was realized by using electron microscopy (SEM, TEM, and EBSD) on the microscopes Tecnai G2 F20 and FEI FEGSEM Qanta 3D (Polish Academy of Science, Krakow, Poland), respectively. Detailed procedure description and its experimental verification were presented by Hilšer et al. in [20,21].

Tensile properties characterization of the investigated magnesium alloy was carried out with the use of Micro-tensile Tests (M-TT). M-TT specimens' geometry and testing procedure was verified by COMTES FHT, Inc. (Pilsen, Czech Republic) in References [22,23]. Testing was performed under quasi-static loading condition at room temperature and ram speed of 0.1 mm/min. The strain was measured with the use of Digital Image Correlation (DIC) system ARAMIS by GOM (COMTES FHT, Inc., Pilsen, Czech Republic). Tests were executed in a servo-hydraulic system with 10 kN capacity under strain rates corresponding to CSN EN 100002-1. Elongation and cross-section reduction were determined on the basis of sample dimensions after test measurement.

The schematic illustration of the M-TT samples and their dimensions and indication of the places for removal small specimens are shown in Figure 3. As it can be seen, the specimens are cut in the longitudinal direction, see Figure 3b.

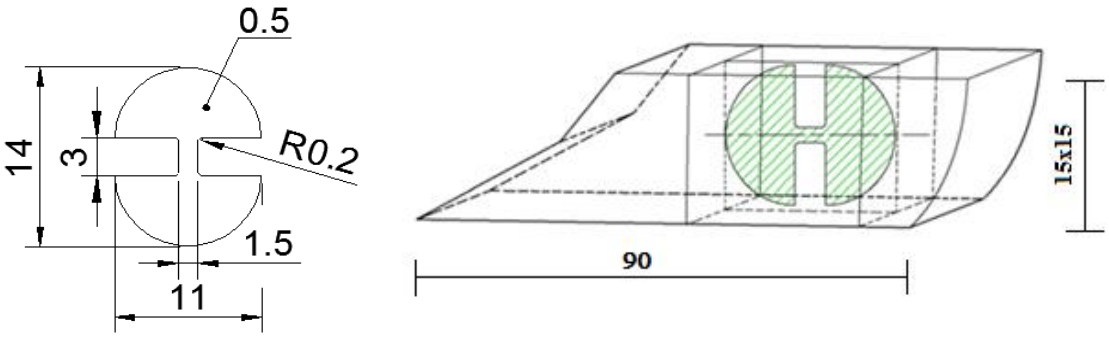

(**a**) (**b**)

Figure 3. The sample prepared for tensile testing: scheme of the specimen (**a**) and scheme of removal of small samples (**b**).

For the M-TT testing, 5 samples were used in each condition. The curves and values are the average of each state.

The schematic illustration of the hardness specimen is presented in Figure 4. The hardness tests according to Vickers HV_5 (load 50 N for 20 s) were carried out on etched metallographic samples. Five specimens were used for hardness evaluation after each state (initial and after individual TCAP passes).

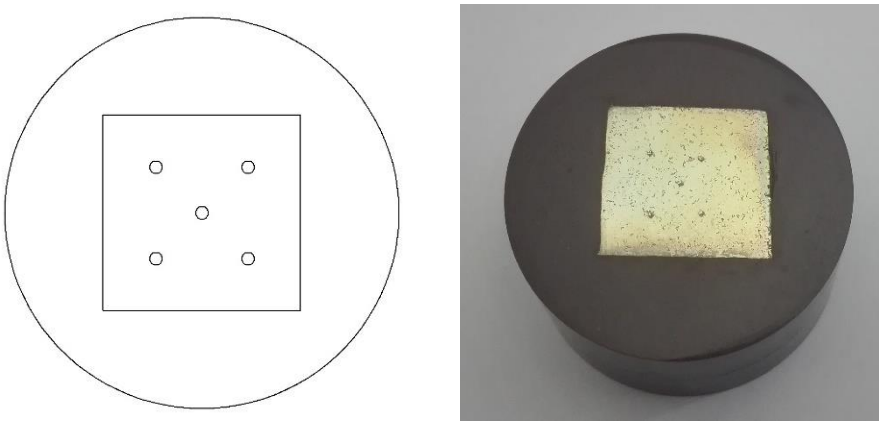

(**a**) (**b**)

Figure 4. The sample prepared for hardness testing: scheme of the specimen (**a**) and real sample (**b**).

4. Experimental Results and Discussion

During TCAP the materials are exposed to severe plastic deformations, which increase with increasing number of passes. During TCAP the real force is monitored by the strain gauge sensor situated on the hydraulic press. This equipment has been used in this work for monitoring the evolution of the force or stress as a function of the displacement.

As mentioned already above, the first indicator of the impact of processing by the TCAP method is the measurement of the evolution of the force/stress on the displacement. Figure 5 shows the stress-displacement curves of one specimen for the first, second, and third pass through the tool with the inserted helix. It is evident from the curve that during the first pass a significant strengthening of the deformed sample (dislocation strengthening) takes place. During the second pass, in the first phase of the TCAP extrusion the sample is stamped into the channel and then the conventional extrusion process continues. The evolution of stress-displacement curves in the second and third passages corresponds to the possibility of dynamical recovery (DRV), or of dynamical recrystallisation (DRX). This conclusion will be further analyzed by microstructural analyses using the transmission electron microscope.

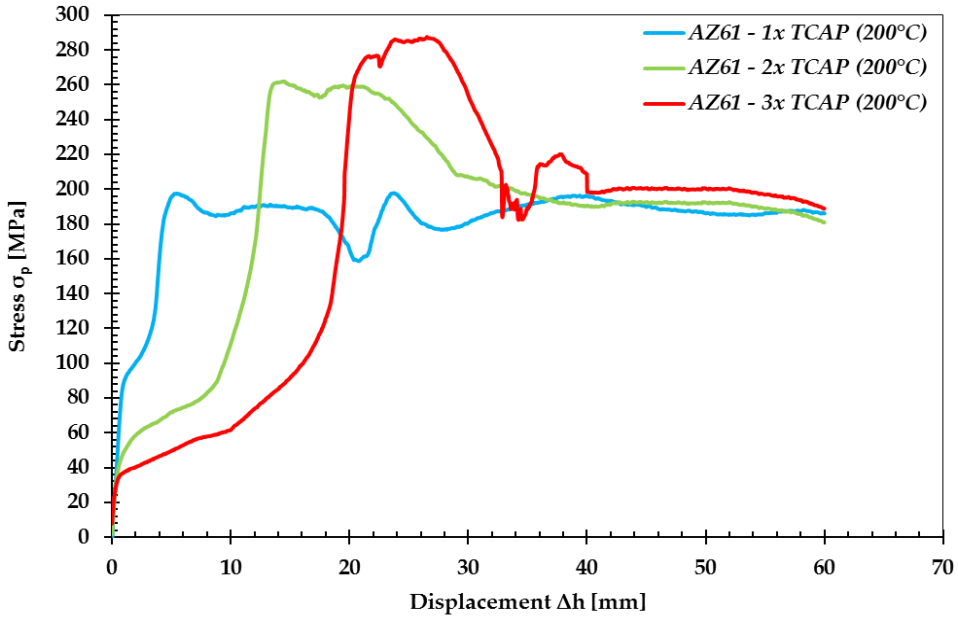

Figure 5. Stress-displacement curves of AZ61 after individual TCAP passes.

4.1. The Microstructure of Magnesium Alloy AZ61

Figure 6 shows the OM images of hot extruded specimens and of those processed by TCAP method. The grain size of the hot extruded state was typically non-uniform on the cross-section and the average grain size was ~24 μm (Figure 6a). The microstructures of samples after TCAP at 200 °C are shown in Figure 5b–d. While many grains were already significantly refined already, just after the first pass, the grain structure was relatively heterogeneous with grains of 9 μm (Figure 6b). The decomposition of the structure attributed to TCAP began in the grain boundary area, in other words, the dynamic recrystallisation began [24], as can be seen in the OM image of the sample after the first pass. After the first pass was grain distribution relatively heterogeneous (microstructure has a bimodal character). Further TCAP passes at the same temperature, a relatively homogeneous microstructure with an average grain size below 2 μm was obtained. This homogeneity after only three passes suggests that original grains were replaced by recrystallized grains (Figure 6c,d).

The OM results will be confirmed by using SEM, TEM, and EBSD observations showing a precise identification of the structural phenomena occurring in the material, both before and after severe plastic deformation by the TCAP method.

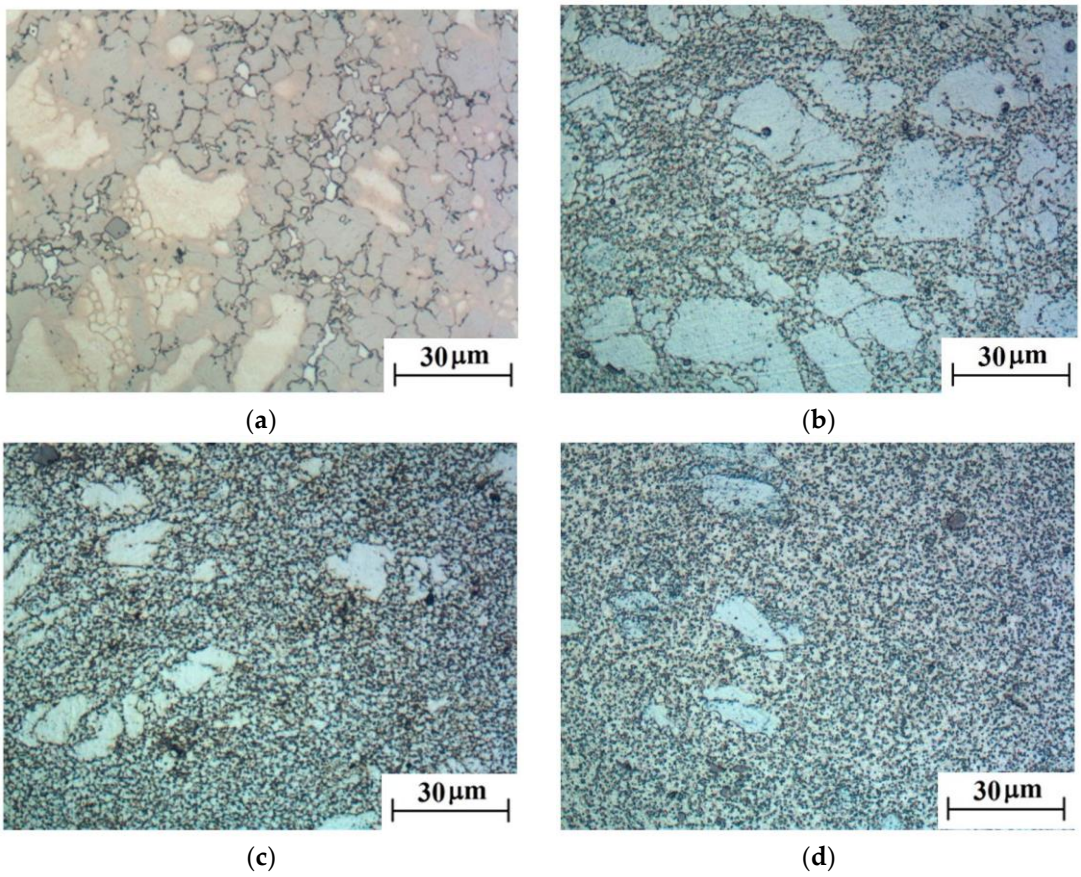

(**a**) (**b**)

(**c**) (**d**)

Figure 6. The OM images of the microstructure of AZ61: Initial (hot extruded) state (**a**); after the first TCAP pass (**b**); after the second TCAP pass (**c**); and after the third TCAP pass (**d**).

Micrograph of the initial state (hot extruded) structure of the investigated magnesium alloy taken in SEM microscope is shown in Figure 7a and the results of the pointwise chemical composition analysis are presented in Figure 7b. The results from EDS analysis confirm that microstructure consists of the following phases: α-Mg, which is a matrix and β-$Mg_{17}Al_{12}$ (separated out at the grain boundaries) and Al_6Mn precipitates. The presence of β-$Mg_{17}Al_{12}$ phase and its effect on the microstructure and properties of Mg-Al-Zn alloys was confirmed by Braszczyńska—Malik in [25,26].

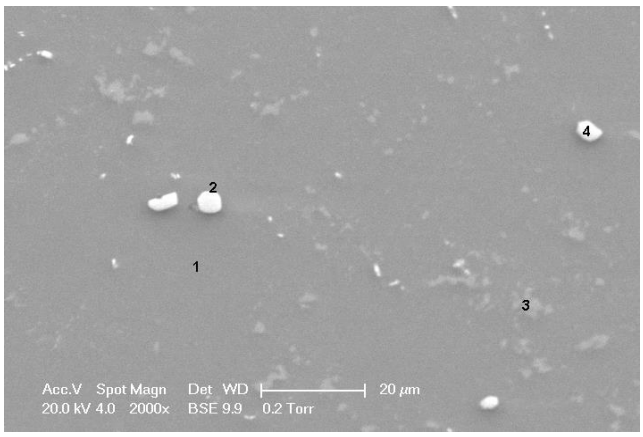

(**a**)

Point	Element	wt.%	at.%
1	MgK	95.37	95.81
	AlK	4.63	4.19
2	MgK	95.04	95.5
	AlK	4.96	4.50
3	MgK	74.47	81.41
	AlK	12.44	12.25
	MnK	13.10	6.34
4	MgK	88.82	89.81
	AlK	11.18	10.19

(**b**)

Figure 7. Initial state microstructure of investigated alloy (**a**) and corresponding pointwise chemical composition analysis (**b**).

TEM investigations of samples after the first and third passes of TCAP were performed in order to examine microstructural features, especially the change of grain size and distribution, but also the size and chemical composition of precipitates. Figure 8 shows the TEM image of hot extruded alloy AZ61 processed by one TCAP pass. It is evident that during the first pass the structure is strongly deformed by shear deformation and deformation twinning (Figure 8b). Average grain size was reduced from initial 24 μm to 5.4 μm. Due to severe plastic deformation, the deformed grains are slightly elongated in the TCAP direction. SADP image shows Mg with the zone exhibiting reflections of severely deformed structure and probably of $Mg_{17}Al_{12}$ precipitates [123].

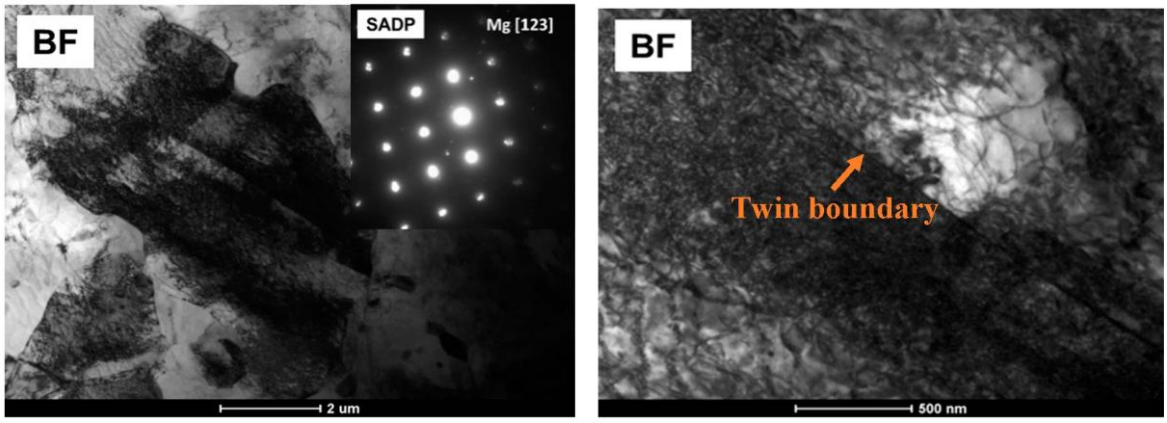

(**a**) (**b**)

Figure 8. Bright Field (BF) with corresponding SADP TEM microstructure of AZ61 alloy after the first pass: dislocations inside deformed grains (**a**) and twins (**b**).

BF microstructures and corresponding SADP of the sample after three passes of TCAP are presented in Figure 9. In this case, a greater refinement of the microstructure can be seen. The average grain size of the sample after the third TCAP pass is below 1.5 μm. Grains with [001] zone have an equiaxed character and lower density of dislocations (compared with TEM after the first pass). These images show a significant role of dynamic recrystallisation (DRX) and grain growth indicated during TCAP realized at 200 °C. Role of static or dynamic recrystallisation on the grain refinement during severe plastic deformation processes was studied in detail by Al-Samman [27] and Sakai in Reference [24], respectively.

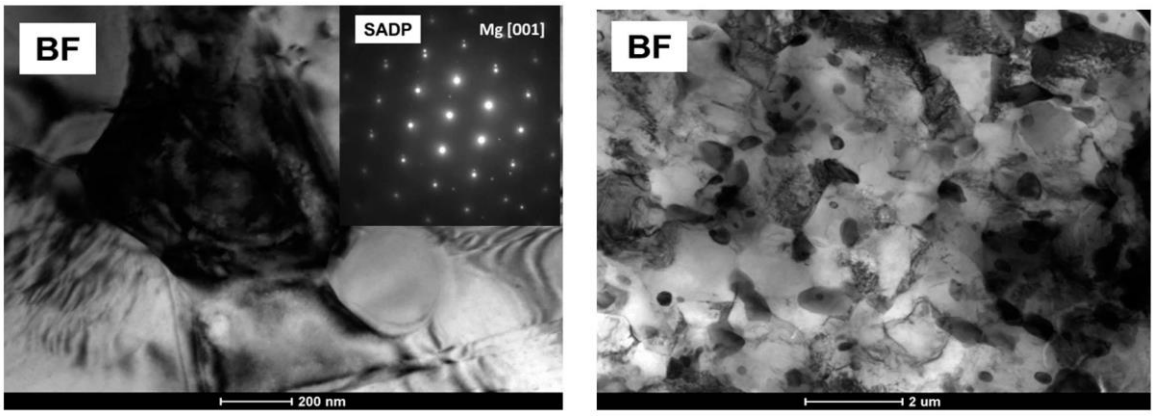

(**a**) (**b**)

Figure 9. BF microstructures and corresponding SADP of the sample after the third pass: different magnifications, scale 200 nm (**a**) and 2 μm (**b**).

Figure 10a presents an EBSD map of the sample after the third pass of TCAP. EBSD analysis results show the same results as those obtained by TEM. The microstructure of AZ61 magnesium alloy consists of fine equiaxed grains, formed by DRX, with only a few elongated grains. The occurrence of small amounts of larger grains with a high density of low angle grain boundaries (LAGB's-red line) with a misorientation angle below 15° is typical for not completely reached dynamic recrystallisation. The HAGB's (black line) are those with a misorientation greater than 15°. The average grain size of the sample after the third pass is below 2 µm (see histogram given in Figure 10b).

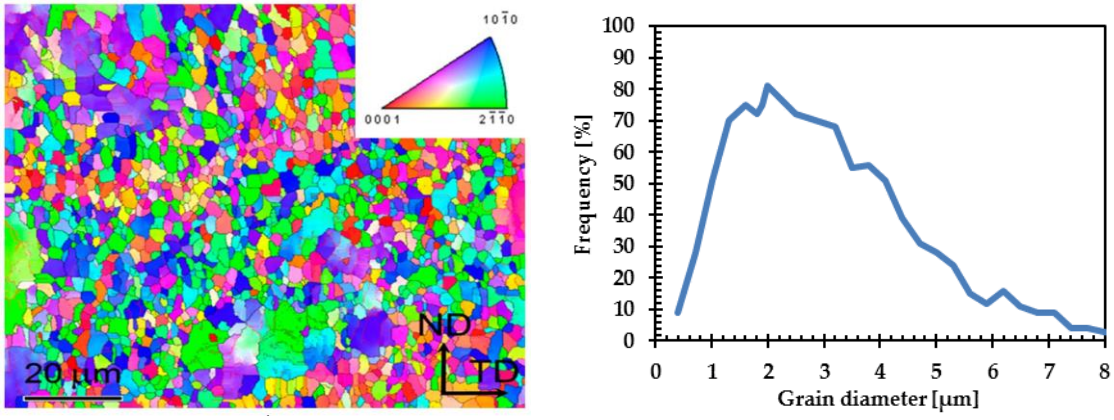

(**a**) (**b**)

Figure 10. Electron backscatter diffraction (EBSD) map of TCAP sample after the third pass with IPF color-coding with respect to TD. Black and red lines indicate high angle grain boundaries (HAGB's) and low angle grain boundaries (LAGB's), respectively (**a**), and corresponding histogram (**b**).

All SADP images apart of reflections originating from magnesium matrix also contain the second network of reflections associated with precipitates. In order to determine the type and distribution of the precipitates, STEM-HAADF investigations were performed. Figure 11 presents a STEM-HAADF image and corresponding elemental maps recorded at the indicated area of the sample after the first pass of TCAP. It is possible to see two types of precipitates in this sample. The first one consists of bigger precipitates containing Al and Mn and the second one consists of smaller precipitates containing Mg, Al, and Zn (Al_6Mn and $MgSi_2$).

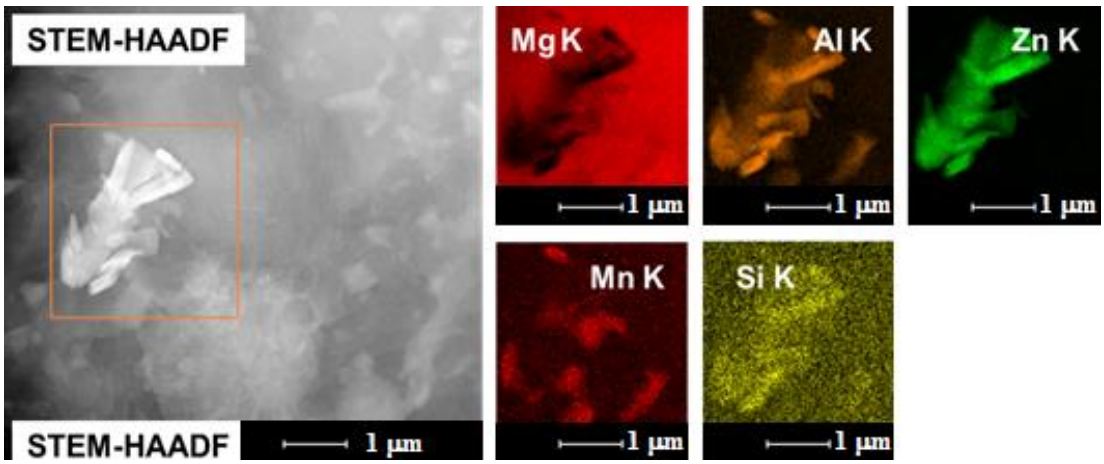

Figure 11. STEM-HAADF image and corresponding elemental maps performed at the marked area of the sample after the first pass.

The precipitates are presented also after three passes of TCAP, however, they differ in size (Figure 12). Especially, the AlMn precipitates are refined and additional manganese is homogeneously

distributed in the magnesium matrix. Moreover, due to the influence of temperature after three passes of TCAP another type of precipitates is formed containing Mg, Al, and Zn. Identification of the crystalline structure of precipitates was performed by use of electron diffraction technique.

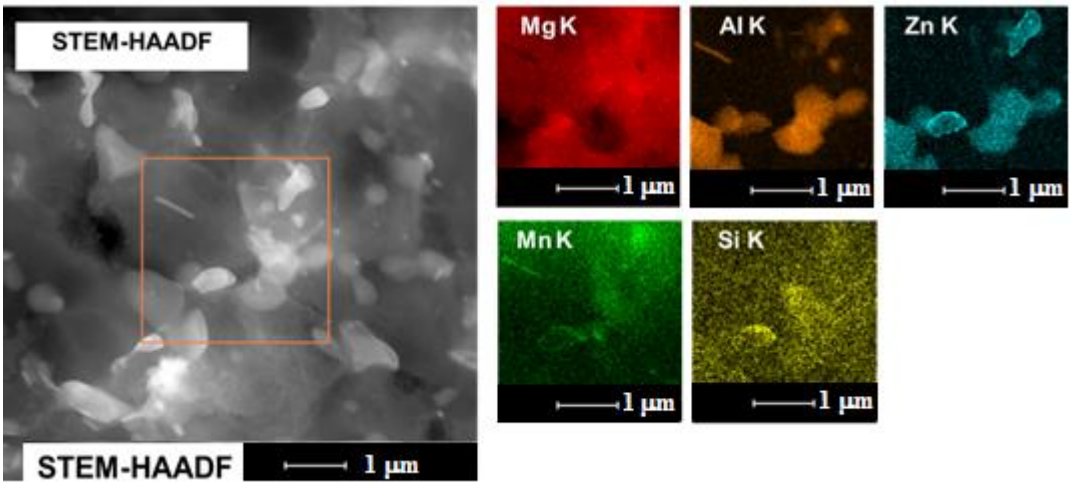

Figure 12. STEM-HAADF image and corresponding elemental maps performed at the marked area of the sample after the third pass.

Figure 13 presents BF images taken at the same magnifications and corresponding SADP of samples after one (a) and three (b) passes, respectively. It can be seen that in the case of the sample after the first pass of TCAP, an irregular precipitate of the $Mg_{17}Al_{12}$ type with the [101] zone axis being located inside the grain with a high density of dislocations and twins. This type of precipitate is mainly present in AZ61 magnesium alloys.

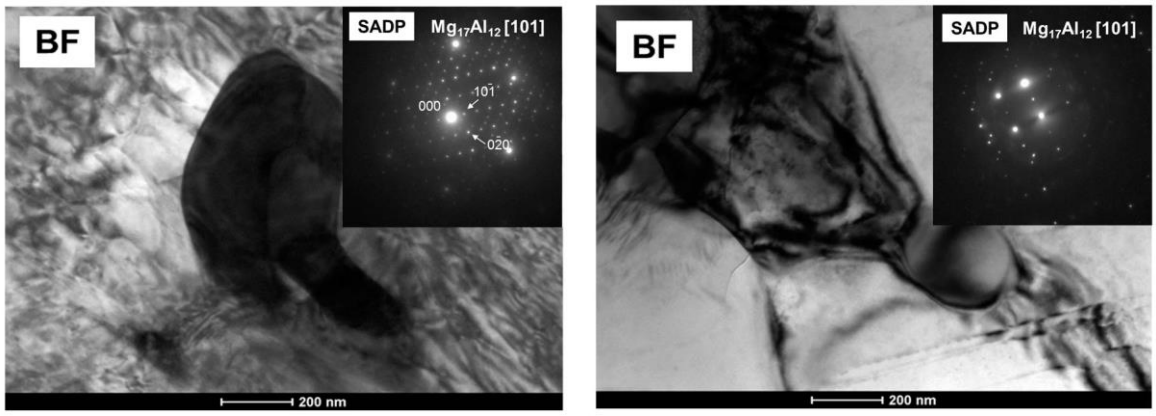

(**a**) (**b**)

Figure 13. BF images with corresponding SADPs of samples after the first (**a**) and the third (**b**) pass by TCAP.

Figure 14 presents TEM image of the sample after the third TCAP pass. From the image of an occurrence of very fine precipitates, localized in grain boundaries area, is evident. At higher magnification the occurrence of defects stacking faults or dislocation pileups between two neighboring $Mg_{17}Al_{12}$ precipitates is evident. Yoshida et al. [28] suggested that after ECAP processing of AZ61 alloy at 175 °C, extremely fine grains with an average grain size of 0.5 µm were formed by dynamic recrystallisation being attributable to dislocation pileups that occurred in the vicinity of dynamically precipitated β-$Mg_{17}Al_{12}$ phase particles with the size of less than 100 nm diameter.

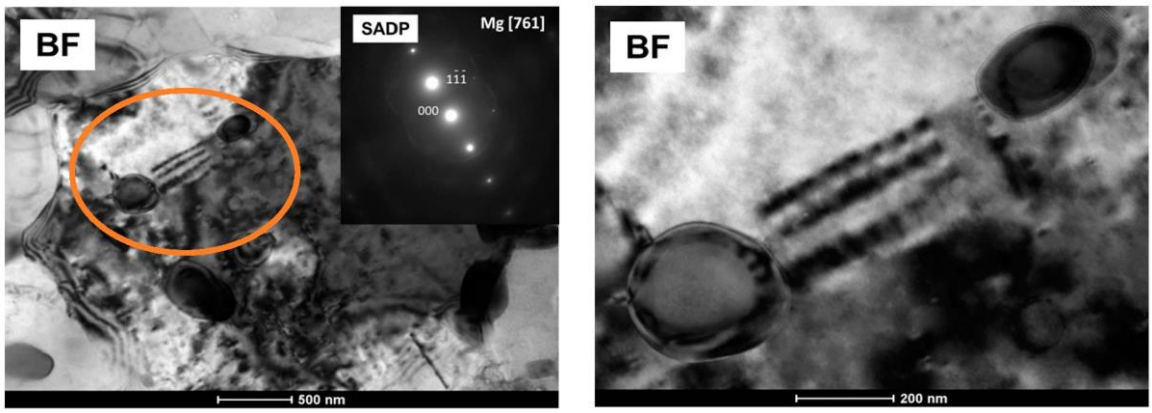

(**a**) (**b**)

Figure 14. BF image at the two different magnifications (**a**) and (**b**) performed in two beam conditions for Mg [761] zone axis in the sample after three passes of TCAP.

The results and model of Mg alloys grain refinement by severe plastic deformation realized at low temperature, presented by Su et al. [29] show that grain refinement mechanism of Mg alloys processed by ECAP is the result of combination of mechanical shearing and subsequent continuous recovery, recrystallisation, and growth of grains and subgrain cells to produce refined and equiaxed grains within the first pass.

The Mg alloy AZ61 subjected to SPD by TCAP possesses the two-phase microstructure consisting of Mg grains of the size close to 1.5 μm after three passes and $Mg_{17}Al_{12}$ precipitates of the size scattered below 200 nm. Grain refinement of the investigated alloy was achieved by a combination of severe plastic deformation with subsequent initiation of dynamic recrystallisation. Grain refinement of the grain size from 24 μm to 1.5 μm was achieved after the third TCAP pass. Thus, it is apparent that Mg-Al-Zn grain refinement is made possible by the interaction of dislocations with recrystallized grains nucleated in the dislocation cells.

4.2. Tensile Properties of AZ61

The original (average) stress-strain curves of investigated magnesium alloy are shown in Figure 15. After the first TCAP pass, the yield stress ($R_{p0.2}$) increased from 199.7 MPa to 235.3 MPa and ultimate tensile strength R_m increased from 261.9 MPa to 321.3 MPa. The strength of the investigated alloy is in good agreement with the results obtained by metallographic analysis. Next passes do not have a significant influence on the strength increase. M-TT results show that strength is increasing only slightly. After the third pass, the values of $R_{p0.2}$ 240.8 MPa and tensile strength R_m 343.6 MPa were achieved (Table 2). Due to the decrease of dislocations density during DRX initiated during TCAP, the plasticity of the experimental alloy increases. TCAP processing improved the elongation to failure from 13.9% (initial state) to 21.4% (after the third TCAP pass).

The results, presented in Table 2, show an increase in the yield stress of approx. 17.8% and of the ultimate tensile strength of approx. 22.6% already just after the first pass by TCAP. Next passes increase the strength only slightly. After the third pass, the yield stress increases by approx. 20.5% and the ultimate tensile strength increases by approx. 31.2%, compared to the initial state. The values of elongation to failure and cross-section reduction increased after the first pass by approx. 21.6% and 27.5%, respectively. Due to dynamic recrystallisation, the elongation increases by approx. 53.9% (compared to the initial state). Cross-section reduction of the samples after the third pass increases only slightly (27.9% compared to the initial state).

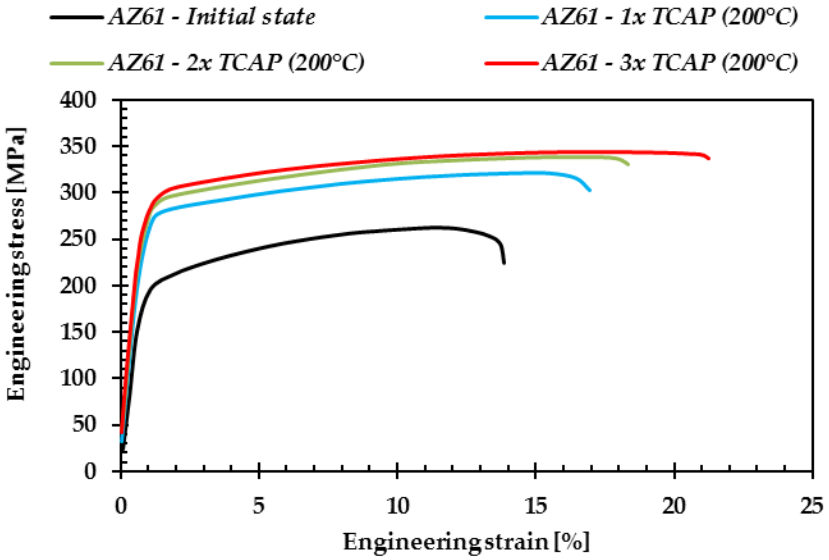

Figure 15. Engineering stress-strain curves of examined samples.

Table 2. Tensile properties and hardness with the standard deviation of the AZ61 magnesium alloy.

Processing Method	$R_{p0.2}$ (MPa)	*R*m (MPa)	*A* (%)	*Z* (%)	HV_5 (-)
Initial state	199.7 ± 9.4	261.9 ± 7.7	13.9 ± 1.3	22.9 ± 1.9	60 ± 3.2
1x TCAP	235.3 ± 5.8	321.3 ± 6.1	16.9 ± 1.2	29.2 ± 1.9	85 ± 2.3
2x TCAP	238.7 ± 1.2	337.9 ± 5.8	18.3 ± 1.1	28.3 ± 1.4	91 ± 1.3
3x TCAP	240.8 ± 0.8	343.6 ± 0.8	21.4 ± 1.1	29.3 ± 0.9	93 ± 0.5

Figure 16 shows an evolution of Vickers hardness HV_5 of investigated alloy with dependence on the number of TCAP passes. The hardness revealed a significant increase after the first pass (about approx. ~42%). Vickers hardness increases with the increasing number of passes, but only slightly.

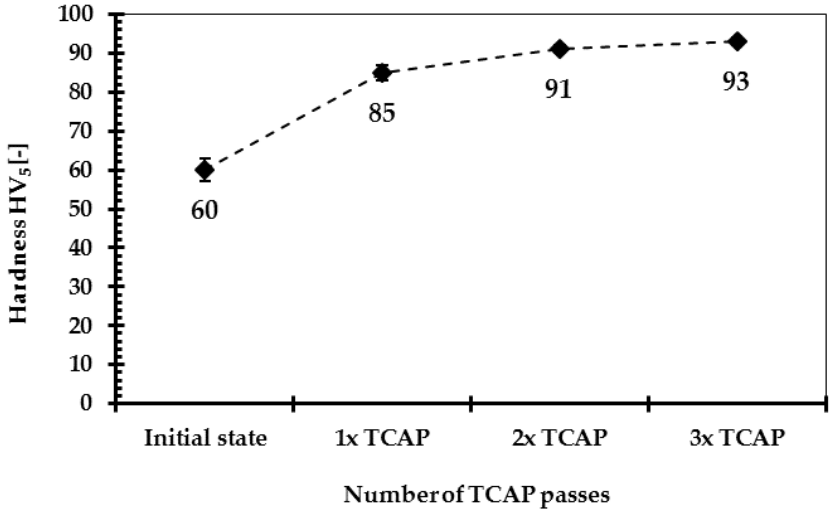

Figure 16. Vickers hardness HV_5 of investigated magnesium alloy AZ61.

It has been agreed that β-$Mg_{17}Al_{12}$ precipitates play a pivotal role in blocking dislocation movements during severe plastic deformation of the investigated alloy. As AZ61 alloy undergoes a TCAP at a process temperature of 200 °C, the $Mg_{17}Al_{12}$ and Al_6Mn phases dissolve in the matrix while fine precipitates will re-precipitate during the following cooling process. After the first pass,

the β phase is replaced by the fine ones, which could considerably reduce local stress concentration and, consequently, postpone the formation of micro-cracks. In addition, apart from the activation of more slip systems during TCAP process, reduction in the influence of $Mg_{17}Al_{12}$ phase usually couples with the dynamic recrystallization, and as a result, significantly improves plasticity.

Yoshida et al. [28] reported the correlation between the grain size and elongation to the failure. They presented that solution treated and ECAPed specimens having average grain size below 8 µm exhibited a high elongation of approx. 33%. This phenomenon was attributed to the dissolution of β precipitates and to the activation of additional deformation mechanisms, such as twinning and GBS.

5. Experimental Results Comparison of TCAP and ECAP Methods

The results of the tensile properties and average grain size of AZ61, subjected to TCAP or ECAP, are given in Table 3.

Table 3. Tensile properties and average grain size of AZ61 magnesium alloy subjected to different SPD methods.

Processing Method	$R_{p0.2}$ (MPa)	Rm (MPa)	A (%)	d_{AVE} (µm)	Reference
E + TCAP (3 × Bc)	240.8	343.6	21.4	1.5	This study
E + ECAP (4 × Bc)	180.3	286.6	17.1	2.5	[30]
HT + ECAP (4 × Bc)	153.2	267.9	12.1	7.9	[31]

Note: E-extrusion, HT-heat treatment (solution treatment), TCAP-twist channel angular pressing, ECAP-equal channel angular pressing.

A good combination of high tensile strength and ductility of AZ61 alloy has been achieved by using TCAP method (compared to conventional ECAP [30,31]). After the four passes by conventional ECAP were achieved the values of yield stress ~180 MPa, the ultimate tensile strength ~287 MPa and elongation ~17%, respectively. As it could be observed that there is not significant increase in alloy subjected to equal channel angular pressing (ECAP) even with solution treatment before ECAP. An analysis of the data given in Table 3 leads to the conclusion that the better tensile properties and grain refinement were obtained by using twist channel angular pressing (TCAP) method.

In comparison with the conventional ECAP it was found that the tensile properties of AZ61 alloy subjected to TCAP process were increased by approx. 34% ($R_{p0.2}$), 20% (R_m) and about 25% (A), respectively. These results are in good agreement with the theoretical conclusions that were presented in this manuscript.

6. Conclusions

The hot extruded AZ61 magnesium alloy was processed by severe plastic deformation method TCAP method using up to three passes at 200 °C. The microstructure and tensile properties were studied using OM, SEM, TEM, EBSD, and micro-tensile testing (M-TT). The following conclusions have been drawn:

- The TEM images of AZ61 magnesium alloy examined after the first pass show an increase of the dislocations density and deformation inside the grains. The results show the significant influence of the forming under SPD conditions on the formation of dislocation substructure and its influence on the tensile properties.
- TEM microstructure of AZ61 magnesium alloy after three passes show Mg matrix microstructure and $Mg_{17}Al_{12}$ precipitate. TEM microstructure of AZ61 alloy after three passes show dislocation structure inside the grain.
- The AZ61 magnesium alloy subjected to SPD by TCAP passes possesses the two-phase microstructure consisting of Mg grains of the size close to 1.5 µm after 3 passes and $Mg_{17}Al_{12}$

precipitates of the size scattered from 100 nm to 200 nm. The primary precipitates of Al_6Mn phase were also observed.

- Refinement of the grain size is probably due to polygonization process associated with the formation of high angle grain boundaries due to the rearrangement of the dislocations and to formation of subgrain structure.
- Micro-tensile tests results show a positive impact of the TCAP method on the increase of the strength properties and plasticity of the investigated magnesium alloy. The M-TT curves show high yield stress and ultimate tensile strength of 240.8 MPa and 343.6 MPa, respectively. Elongation to the failure of the sample after 3 passes by TCAP method reaches 21.4%.

Based on microstructural and M-TT analyses results presented in this paper it can be concluded that severe plastic deformation induced by TCAP has a significant influence on the grain refinement and on the increase in strength properties while preserving plasticity of the investigated magnesium alloy AZ61.

Author Contributions: O.H. performed forming process, hardness measurement and analyzed the data; S.R. supervised the experimental work; P.S. wrote the paper; L.Č. performed metallographic experiments on OM and analyzed the results; J.D. performed M-TT tests and analyzed the results; W.M. performed metallographic analysis on electron microscope (SEM, TEM and EBSD) and analyzed the obtained results and supervised the paper; M.K. supervised and reviewed the paper; All authors discussed the paper.

Funding: This paper was created within the projects Ministry of Education, Youth and Sports of Czech Republic for its support to the project "Pre-seed Materials IA3, Production technology of a sheet strip with an ultra-fine grain structure", No. CZ.1.05/3.1.00/14.0320, project "Technological design and project management of production and material systems" No. SP2018/67 and project "Creation of an international team of scientists and participation in scientific networks in the sphere of nanotechnology and unconventional forming material" CZ.1.07/2.3.00/20.0038.

Conflicts of Interest: The authors declare no conflict of interest.

References

1. Avedesian, M.; Baker, H. *ASM Speciality Handbook: Magnesium and Magnesium Alloys*, 2nd ed.; ASM International: Geauga County, OH, USA, 1999; p. 350, ISBN 978-0-87170-657-7.
2. Mordike, B.L.; Ebert, T. Magnesium: Properties-Application-Potential. *Mater. Sci. Eng. A* **2001**, *302*, 37–45. [CrossRef]
3. Friedrich, H.E.; Mordike, B.L. *Magnesium Technology: Metallurgy, Design Data, Applications*, 1st ed.; Springer: Berlin/Heidelberg, Germany, 2006; p. 677, ISBN 978-3-54020-599-9.
4. Somekawa, H.; Singh, A.; Sahara, R.; Inoue, T. Excellent room temperature deformability in high strain rate regimes of magnesium alloy. *Sci. Rep.* **2018**, *8*, 656. [CrossRef] [PubMed]
5. Čížek, L.; Rusz, S.; Hilšer, O.; Śliwa, R.; Kuc, D.; Tański, T.; Tkocz, M. Microstructure and properties of selected magnesium-aluminium alloys prepared for SPD processing technology. *Arch. Metall. Mater.* **2017**, *62*, 2365–2370. [CrossRef]
6. Wang, X.J.; Xu, D.K.; Wu, R.Z.; Chen, X.B.; Peng, Q.M.; Jin, L.; Xin, Y.C.; Zhang, Z.Q.; Liu, Y.; Chen, X.H.; et al. What is going on in magnesium alloys? *J. Mater. Sci. Technol.* **2018**, *34*, 245–247. [CrossRef]
7. Hilšer, O.; Rusz, S.; Maziarz, W.; Dutkiewicz, J.; Tański, T.; Snopiński, P.; Džugan, J. Structure and properties of AZ31 magnesium alloy after combination of hot extrusion and ECAP. *Acta Metall. Slov.* **2017**, *23*, 222–228. [CrossRef]
8. Vinogradov, A.; Estrin, Y. Analytical and numerical approaches to modelling severe plastic deformation. *Prog. Mater. Sci.* **2018**, *95*, 172–242. [CrossRef]
9. Tański, T.; Snopiński, P.; Pakieła, W.; Borek, W.; Prusik, K.; Rusz, S. Structure and properties of AlMg alloy after combination of ECAP and post-ECAP ageing. *Arch. Civ. Mech. Eng.* **2016**, *16*, 325–334. [CrossRef]
10. Mavlyutov, A.M.; Orlova, T.S.; Latynina, T.A.; Kasatkin, I.A.; Murashkin, M.Y.; Valiev, R.Z. Influence of additional deformation on microstructure, mechanical and electrical properties of Al-Mg-Si alloy processed by high pressure torsion. *Rev. Adv. Mater. Sci.* **2017**, *52*, 61–69.

11. Trojanová, Z.; Džugan, J.; Halmešová, K.; Németh, G.; Minárik, P.; Lukáč, P.; Bohlen, J. Influence of accumulative roll bonding on the texture and tensile properties of an AZ31 magnesium alloy sheets. *Materials* **2018**, *11*, 73. [CrossRef] [PubMed]
12. Zhang, L.; Wang, Q.; Liu, G.; Guo, W.; Ye, B.; Li, W.; Jiang, H.; Ding, W. Tribological behaviour of carbon nanotube-reinforced AZ91D composites processed by cyclic extrusion and compression. *Tribol. Lett.* **2018**, *66*, 71. [CrossRef]
13. Bazarnik, P.; Huang, Y.; Lewandowska, M.; Langdon, T.G. Enhanced grain refinement and microhardness by hybrid processing using hydrostatic extrusion and high-pressure torsion. *Mater. Sci. Eng. A* **2018**, *712*, 513–520. [CrossRef]
14. Chang, S.Y.; Lee, S.W.; Kang, K.M.; Kamodo, S.; Kojima, Y. Improvement of mechanical characteristics in severely plastic-deformed Mg alloys. *Mater. Trans.* **2004**, *45*, 488–492. [CrossRef]
15. Palán, J.; Maleček, L.; Hodek, J.; Zemko, M.; Džugan, J. Possibilities of biocompatible material production using conform SPD technology. *Arch. Mater. Sci. Eng.* **2017**, *88*, 5–11. [CrossRef]
16. Beygelzimmer, Y.; Kulagin, R.; Estrin, Y.; Toth, L.S.; Kim, H.S.; Latypov, M.I. Twist extrusion as a potent tool for obtaining advanced engineering materials: A review. *Adv. Eng. Mater.* **2017**, *19*, 1600873. [CrossRef]
17. Rusz, S.; Tylšar, S.; Kedroň, J.; Dutkiewicz, J.; Donič, T. Enhancement of efficiency of SPD process by application of new geometry of ECAP tool. *Acta Metall. Slov.* **2010**, *16*, 229–236.
18. Kocich, R.; Greger, M.; Kursa, M.; Szurman, I.; Macháčková, A. Twist channel angular pressing (TCAP) as a method for increasing the efficiency of SPD. *Mater. Sci. Eng. A* **2010**, *527*, 6386–6392. [CrossRef]
19. Snopiński, P.; Tański, T.; Labisz, K.; Rusz, S.; Jonšta, P.; Król, M. Wrought aluminium-magnesium alloys subjected to SPD processing. *Int. J. Mater. Res.* **2016**, *107*, 637–645. [CrossRef]
20. Rusz, S.; Salajka, M.; Čížek, L.; Tylšar, S.; Kedroň, J. Metallographic analysis of ECAP processed selected magnesium alloys. In *Materials Science Forum, Proceedings of the International Symposium on Metallography, Stará Lesná, Slovakia, 24–26 April 2013*; Trans Tech Publications Ltd.: Stará Lesná, Slovakia, 2013; Volume 782. [CrossRef]
21. Hilšer, O.; Rusz, S.; Tański, T.; Snopiński, P.; Džugan, J.; Kraus, M. Mechanical properties and structure of AZ61 magnesium alloy processed by equal channel angular pressing. In *IOP Conference Series: Materials Science and Engineering, Proceedings of the 4th International Conference Recent Trends in Structural Materials, COMAT 2016, Angelo Hotel, Pilsen, Czech Republic, 9–11 November 2016*; Tanger Ltd.: Ostrava, Czech Republic, 2017. [CrossRef]
22. Konopík, P.; Džugan, J.; Rund, M.; Procházka, R. Determination of local mechanical properties of metal components by hot micro-tensile test. In Proceedings of the 25th Anniversary International Conference on Metallurgy and Materials, METAL 2016, Hotel Voroněž, Brno, Czech Republic, 25–27 May 2016.
23. Džugan, J.; Rund, M.; Prantl, A.; Konopík, P. Mini-tensile specimen application for sheets characterization. In *IOP Conference Series: Materials Science and Engineering, Proceedings of the 4th International Conference Recent Trends in Structural Materials, COMAT 2016, Angelo Hotel, Pilsen, Czech Republic, 9–11 November 2016*; Tanger Ltd.: Ostrava, Czech Republic, 2017. [CrossRef]
24. Sakai, T.; Belyakov, A.; Kaibyshev, R.; Miura, H.; Jonas, J.J. Dynamic and post-dynamic recrystallization under hot, cold and severe plastic deformation conditions. *Prog. Mater. Sci.* **2014**, *60*, 130–207. [CrossRef]
25. Braszczyńska-Malik, K.N. Spherical shape of γ-$Mg_{17}Al_{12}$ precipitates in AZ91 magnesium alloy processed by equal-channel angular pressing. *J. Alloys Comp.* **2009**, *487*, 263–268. [CrossRef]
26. Braszczyńska-Malik, K.N. Discontinuous and continuous precipitation in magnesium-aluminium type alloys. *J. Alloys Comp.* **2009**, *477*, 870–876. [CrossRef]
27. Al-Samman, T.; Gottstein, G. Dynamic recrystallization during high temperature deformation of magnesium. *Mater. Sci. Eng. A* **2008**, *490*, 411–420. [CrossRef]
28. Yoshida, Y.; Arai, K.; Itoh, S.; Kamado, S.; Kojima, Y. Realization of high strength and ductility for AZ61 magnesium alloy by severe warm working. *Sci. Technol. Adv. Mater.* **2005**, *6*, 185–194. [CrossRef]
29. Su, C.W.; Lu, L.; Lai, M.O. A model for grain refinement mechanism in equal channel angular pressing of Mg alloy from microstructural studies. *Mater. Sci. Eng. A* **2006**, *434*, 227–236. [CrossRef]

30. Vinogradov, A.; Serebryany, V.N.; Dobatkin, S.V. Tailoring microstructure and properties of fine grained magnesium alloys by severe plastic deformation. *Adv. Eng. Mater.* **2017**, *20*, 22. [CrossRef]
31. Xie, Q.; Ma, A.; Jiang, J.; Cheng, Z.; Song, D.; Yuan, Y.; Liu, H. Stress corrosion cracking behavior of fine-grained AZ61 magnesium alloys processed by equal-channel angular pressing. *Metals* **2017**, *7*, 343. [CrossRef]